III International Symposium

TOPICAL PROBLEMS OF BIOPHOTONICS

PLENARY TALKS

OCT AND DEPTH RESOLVED FLUORESCENCE ENDOSCOPY

J.F. de Boer, M. de Groot, and **J. Li**

Institute Laserlab, Department of Physics and Astronomy, VU University, Amsterdam. The Netherlands
E-mail: jfdeboer@few.vu.nl

Optical Coherence Tomography is a minimally invasive optical technique to create high resolution cross sectional images of tissue. The advance of Spectral/Fourier domain OCT techniques have enabled high speed data acquisition and volumetric imaging within short times. Fourier/Spectral domain OCT is hugely successful in ophthalmology, with more than seven companies commercializing the technique. The success in ophthalmology can be attributed to the ability of OCT to show the morphological structure of the retina in great detail. In cardiology several companies are expected to enter the market for imaging of the coronary arteries. The aforementioned applications have in common that the diagnostic criteria can be based on morphological or structural changes in the tissue. The application of OCT for the characterization and diagnosis of cancer however is still in its infancy. OCT is capable of visualizing structural changes and tissue abnormalities. The main hurdle that OCT faces is the limited structural contrast between benign and malignant lesions. Several extensions to OCT can improve the contrast, the main ones being Doppler OCT and Polarization sensitive OCT. Doppler OCT can visualize the blood vessel structure associated with angiogenesis promoted by tumors. Polarization OCT provides contrast by measuring the polarization state changes of light in the tissue. Most fibrous tissues like muscle, nerve and collagen exhibit birefringence, which changes the polarization state of light. Tumors break down the extracellular matrix, including collagen. Thus polarization sensitivity provides an indication of the collagen density and the state of the extracellular matrix.

The majority of cancers develop in the epithelial lining of tissue. The epithelial lining of hollow organs can be accessed by small endoscopes. In order to image these locations, OCT endoscopes need to be developed that are small, and have a circumferential scan pattern. Most OCT catheters provide the circumferential scan pattern by a motor proximal to the endoscope, where the rotational motion is transferred to the endoscope tip by a drive shaft. A rotary junction is necessary to couple the rotating light guiding fiber to a stationary one. Development of rotary junction becomes increasingly difficult for optical fibers more complicated than single core fibers. We will present a miniature endoscope with a motor at the distal end of the catheter, avoiding the use of a rotary junction. The use of a distal motor allows the use of multicore fibers that would allow the integration of OCT with fluorescent techniques.

Just as fluorescence has revolutionized cell biology, it is expected to have a major impact on clinical medicine. This development is at its infancy, but insight into its possible application can be gained from the field of immuno-PET, where monoclonal antibodies (MAbs) are conjugated with PET tracers for diagnostic purposes and the evaluation of potential treatments. Immuno-fluorescence (conjugating a MAb with a fluorescent molecule) is equivalent to immuno-PET, but requires catheters or endoscopes to detect the fluorescence close to the emitting source. In order to gain depth information, a depth scanning mechanism needs to be developed that is compatible with small catheters or endoscopes. We have developed an interferometric technique, Self Interference Fluorescence Endoscopy (SIFE) that allows generation of depth dependent fluorescence without a scan mechanism at the distal end of the catheter, permitting miniaturization of the catheter.

We will present a miniature catheter with a distal micromotor for circumferential scanning OCT with an outer diameter of 1.65 mm. The principle of SIFE and preliminary results will be presented. We will show that the catheter can be used to detect depth resolved fluorescence simultaneously with the OCT structural information.

Acknowledgements

The research was supported by the National Institute of Health (R21 RR023139) and the dutch foundation for fundamental research (FOM-NIG, and ZonMW).

ULTRAMICROSCOPY: 3D-RECONSTRUCTION OF DROSOPHILA'S INNER ANATOMY WITH IMPROVED OPTICS

H.U. Dodt, N. Jährling, S. Saghafi, and **K. Becker**

Chair of Bioelectronics, Institute of Solid State Electronics, TU Vienna, Vienna, Austria
dodt@tuwien.ac.at

Ultramicroscopy – a light sheet based microscopy technique has various applications in biological research. In the first generation ultramicroscope the light sheet was generated by an optical system consisting of a slit aperture and a single cylindrical lens placed in front of the aperture. A semi-uniform intensity distribution is produced through the truncation of an expanded Gaussian beam. The cylindrical lens focuses the truncated beam in one direction, whilst being relatively unchanged in the perpendicular direction. Although a light sheet generated in this way can be very thin close to its focal point, it diverges rapidly with increasing distance. The slope of this broadening is quantitatively described by the Rayleigh range. The uniformity of the laser intensity along the line of focus, and the length of this line are critical issues in ultramicroscopy. The optical characteristics of a light sheet, i.e. Rayleigh range, power density and beam width, are dependent on the size of the slit aperture. Large aperture would produce a light sheet that is very pinched at its focus, but which promptly diverges both behind and in front of the focal area. This results in a short Rayleigh range and reduced uniformity along the propagation axis of the light sheet. Using a smaller aperture extends the Rayleigh range, yet inevitably increases the thickness of the light sheet. Furthermore, there will be a major loss in the illumination power. We present an improved optical setup, applying a combination of one plano-concave lens, and three cylindrical lenses, placed in parallel- and crossed-axis positions. This configuration enables us to produce a thin sheet of light with a small beam diameter at the focus (comparable to a large aperture system), whilst providing a longer Rayleigh range (as produced in a small aperture system). Additionally, the power loss is significantly reduced by up to 50%. We quantitatively analyzed the light sheets generated by the new and the standard optical system, using theoretical and experimental approaches. Both models are compared, theoretically and experimentally, with respect to their ability to improve the resolution of fine details in ultramicroscopy.

Drosophila is an important model organism for studying the function of genes linked to neuro-degenerative diseases Recent developments of RNAi libraries allow the systematic, genome-wide analysis of Drosophila tissue morphogenesis. To phenotype the large numbers of fly mutants generated this way, sophisticated microscopy techniques are required. These techniques ideally should allow the 3D-reconstruction of the inner anatomy including the nervous system of an entire fly from a single scan. Unfortunately, Drosophila is too large to image the entire fly by standard confocal microscopy in a single pass. Hence, the fly has to be sliced mechanically before microscopic inspection. This unavoidably produces artifacts, such as mechanical distortions and misalignments. Ultramicroscopy, allows optical sectioning of microscopic specimens up to several cm in size, whilst providing micron resolution. By using a thin sheet of laser light for optical sectioning it makes mechanical slicing unnecessary even in very large specimen. This also provides a striking advance in speed. Recording a whole fly with ultramicroscopy takes about 30 min, including 3D reconstruction.

We present ultramicroscopy reconstructions of the flight musculature, the nervous system, and the digestive tract of entire, chemically cleared Drosophila in autofluorescent light. From these reconstructions segmentations of different organ systems were obtained. Our method provides reliable 3D reconstructions of relatively large structures, such as the indirect flight muscles, whilst even the very filigree organization of the direct flight muscles is spatially resolved. Due to its speed and convenience, ultramicroscopy may become a valuable tool for the morphological analysis of fly mutants.

References

1. H.U. Dodt et al., *Nat. Methods*, 2007, **4**, 331-336.
2. K. Becker, N. Jährling, E.R. Kramer, F. Schnorrer, and H.U. Dodt, *J. Biophot*., 2008, **1**, 36-42.
3. N. Jährling, K. Becker, E.R. Kramer, and H.U. Dodt, *Med. Laser Appl*., 2008, **4**, 209-215.
4. N. Jährling, K. Becker, C. Schönbauer, F. Schnorrer, and H.U. Dodt, *Front. Neurosci.*, 2010, **4**, 1-5.

BED-SIDE TRANSCRANIAL OPTICAL MONITORS FOR NEURO-INTENSIVE CARE MONITORING

T. Durduran

ICFO- Institut de Ciències Fotòniques, Mediterranean Technology Park, 08860 Castelldefels (Barcelona), Spain
Tel: 34-93-553-4151, Fax: 34-93-553-4000, E-mail: turgut.durduran@icfo.es

Transcranial, non-invasive monitoring of cerebral hemodynamics, autoregulation and metabolism at the neuro-intensive care has a great deal of potential for improving the clinical management of conditions such as stroke and traumatic brain injury. Hybrid diffuse optical and correlation spectroscopies are emerging as promising tools to this end. Basics of the technologies and the latest clinical studies are presented.

The development of diffuse correlation spectroscopy (DCS) (also known as "diffuse wave spectroscopy") for non-invasive measurement of cerebral blood flow (CBF) in human brain is outlined [1]. DCS for deeptissue, biomedical monitoring and imaging was developed at the laboratory of the University of Pennsylvania, Philadelphia, USA starting from a theoretical development and then leading to clinical pilot studies. By combining DCS with simultaneous diffuse optical spectroscopy (DOS), changes in cerebral blood flow (rCBF), oxy-hemoglobin (rHbO2) and deoxy-hemoglobin (rHb) concentrations and total hemoglobin concentration (rTHC) are measured. This enables calculation of changes in metabolic rate of oxygen (rMRO2). Early work on brain focused on theory [2] and experiments on rat brains [3] where we obtained images during transient ischemia [4] and cortical spreading depression [5, 6]. Later, the method's capability to non-invasively measure global and local changes in response to functional stimuli in adult human brain [7–9] was demonstrated.

Over the last few years, the technology was developed towards the clinical implementation of portable, bedside monitors that are usable at the harsh environment of intensive care units. Its feasibility on critically ill patients was demonstrated in stroke patients [10], in traumatic brain injury patients [11], cardiac patients [12] and in both premature [13, 14] and term neonates [15]. The technique has now been tested on hundreds of volunteers and patients and was validated against a multitude of modalities [1]. It has been adopted by other laboratories in other laboratories in USA [14, 16, 17], Germany [9], Canada [18], Spain [19] and reports are starting to appear from other places.

In this presentation, I describe the development of these monitors, explain how various challenges were overcome, demonstrate their accuracy through validation studies against laser Doppler flowmetry, color Doppler ultrasound, transcranial Doppler ultrasound, arterial spin labeled magnetic resonance imaging, invasive fluorescent microspheres, portable xenon enhanced computer tomography and against oxygen electrodes. We show studies extending to continuous acquisition periods of ~12 hours. Specific patient populations include sufferers of acute ischemic stroke, hemorrhagic stroke, traumatic brain injury, congenital heart defects and very low birth-weight premature birth.

Overall, these studies demonstrate hybrid optical techniques as promising techniques for use as bed-side monitors. More complete information about cerebral physiology is now accessible with the addition of cerebral blood flow measurements and the ability to estimate cerebral oxygen metabolism. Assessment of cerebral autoregulation is proposed as a potentially useful quantity for individualized neuro-intensive care.

This work was partially funded by Fundaciò Cellex Barcelona, Marie Curie IRG (FP7-PEOPLE-2009-RG: 249223 RPTAMON) and Instituto de Salud Carlos III (FIS). It is the product of many years of collaborations with many faculty, researchers and students from University of Pennsylvania and Children's Hospital of Philadelphia. In particular, Dr Arjun Yodh, Dr John Detre, Dr Joel Greenberg and Dr Daniel Licht have been the leaders of this effort.

References

1. T. Durduran, R. Choe, W. Baker, and A.G. Yodh, "Diffuse optics for tissue monitoring and tomography", *Rep. Prog. Phys.*, **73**(7), 2010.
2. D.A. Boas, L.E. Campbell, and A.G. Yodh, "Scattering and imaging with diffusing temporal field correlations", *Phys. Rev. Lett.*, 1995, **75**(9), 1855–1858.
3. C. Cheung, J.P. Culver, K. Takahashi, J.H. Greenberg, and A.G. Yodh, "*In vivo* cerebrovascular measurement combining diffuse near-infrared absorption and correlation spectroscopies", *Phys. Med. and Biol.*, 2001, **46**(8), 2053–2065.
4. J.P. Culver, T. Durduran, D. Furuya, C. Cheung, J.H. Greenberg, and A.G. Yodh, "Diffuse optical tomography of cerebral blood flow, oxygenation and metabolism in rat during focal ischemia", *J. Cereb. Blood Flow Metab.*, 2003, **23**, 911–24.
5. T. Durduran, "Non-Invasive Measurements of Tissue Hemodynamics with Hybrid Diffuse Optical Methods", *Ph.D. Dissertation, University of Pennsylvania*, 2004.
6. C. Zhou, G. Yu, D. Furuya, J.H. Greenberg, A.G. Yodh, and T. Durduran, "Diffuse optical correlation tomography of cerebral blood flow during cortical spreading depression in rat brain", *Opt. Exp.*, 2006, **14**, 1125–44.
7. T. Durduran, G. Yu, M.G. Burnett, J.A. Detre, J.H. Greenberg, J. Wang, C. Zhou, and A.G. Yodh, "Diffuse optical measurements of blood flow, blood oxygenation and metabolism in human brain during sensorimotor cortex activation", *Opt. Lett*, 2004, **29**, 1766–1768.
8. C. Zhou, "*In-Vivo* Optical Imaging and Spectroscopy of Cerebral Hemodynamics", *Ph.D. Dissertation, University of Pennsylvania*, 2007.
9. J. Li, G. Dietsche, D. Iftime, S.E. Skipetrov, G. Maret, T. Elbert, B. Rockstroh, and T. Gisler, "Noninvasive detection of functional brain activity with near-infrared diffusing-wave spectroscopy", *J. Biomed. Opt.*, Jul-Aug 2005, **10**(4), 044002–1–044002–12.
10. T. Durduran, C. Zhou, B.L. Edlow, G. Yu, R. Choe, M.N. Kim, B.L. Cucchiara, M.E. Putt, Q. Shah, S.E. Kasner, J.H. Greenberg, A.G. Yodh, and J.A. Detre, "Transcranial optical monitoring of cerebrovascular hemodynamics in acute stroke patients", *Optics Express*, 2009, **17**(5), 3884–3902.
11. M.N. Kim, T. Durduran, S. Frangos, B.L. Edlow, E.M. Buckley, E.M. Heather, C. Zhou, G. Yu, R. Choe, E. Maloney-Wilensky, R.L. Wolf, J.H. Woo, M.S. Grady, J.H. Greenberg, J.M. Levine, A.G. Yodh, J.A. Detre, and W.A. Kofke, "Noninvasive measurement of cerebral blood flow and blood oxygenation using near-infrared and diffuse correlation spectroscopies in critically brain-injured adults", *Neurocritical Care*, April 2010, **12**(2), 173–180.
12. Y. Shang, R. Cheng, L. Dong, S.J. Ryan, S.P. Saha, and G. Yu. "Cerebral monitoring during carotid endarterectomy using near-infrared diffuse optical spectroscopies and electroencephalogram", *Physics in Medicine and Biology*, 2011, **56**, 3015.
13. E.M. Buckley, N.M. Cook, T. Durduran, M.N. Kim, C. Zhou, R. Choe, Yu. Guoqiang, S. Shultz, C.M. Sehgal, D.J. Licht, P.H. Arger, M.E. Putt, H.H. Hurt, and A.G. Yodh, "Cerebral hemodynamics in preterm infants during positional intervention measured with diffuse correlation spectroscopy and transcranial doppler ultrasound", *Optics Express*, 2009, **17**, 12571–12581.
14. N. Roche-Labarbe, S.A. Carp, A. Surova, M. Patel, D.A. Boas, P.E. Grant, and M.A. Franceschini, "Noninvasive optical measures of cbv, sto2, cbf index, and rcmro2 in human premature neonates' brains in the first six weeks of life (p na)", *Human Brain Mapping*, 2009, **31**(3), 341–352.
15. T. Durduran, C. Zhou, E.M. Buckley, M.N. Kim, G. Yu, R. Choe, W.J. Gaynor, T.L. Spray, S.M. Durning, S.E. Mason, L.M. Montenegro, S.C. Nicolson, R.A. Zimmerman, M.E. Putt, J.J. Wang, J.H. Greenberg, J.A. Detre, A.G. Yodh, and D.J. Licht, "Optical measurement of cerebral hemodynamics and oxygen metabolism in neonates with congenital heart defects", *J. Biomed. Opt.*, May/June 2010, **15**(3), 037004.
16. U. Sunar, D. Rohrbach, N. Rigual, E. Tracy, K. Keymel, M.T. Cooper, H. Baumann, and B.H. Henderson, "Monitoring photobleaching and hemodynamic responses to hpph-mediated photodynamic therapy of head and neck cancer: a case report", *Opt. Express*, 2010, **18**(14), 14969–14978.
17. Y. Shang, Y. Zhao, R. Cheng, L. Dong, D. Irwin, and G. Yu, "Portable optical tissue flow oximeter based on diffuse correlation spectroscopy", *Optics Letters*, 2009, **34**(22), 3556–3558.
18. L. Gagnon, M. Desjardins, J. Jehanne-Lacasse, L. Bherer, and F. Lesage, "Investigation of diffuse correlation spectroscopy in multi-layered media including the human head", *Opt. Express*, 2008, **16**(20), 15514–15530.
19. P. Zirak, R. Delgado-Mederos, J. Martí–Fàbregas, and T. Durduran, "Effects of acetazolamide on the micro- and macrovascular cerebral hemodynamics: A diffuse optical and transcranial doppler ultrasound study", *Biomedical Optics Express*, December 2010, **1**(5), 1443–1459.

IN VIVO INVESTIGATION OF ASTROCYTIC DYNAMICS BY IMAGING AND ELECTROPHYSIOLOGY

H. Hirase

RIKEN – Brain Science Institute, Wako, Japan, hirase@brain.riken.jp;
Saitama University, Brain Science Institute, Saitama, Japan

Introduction. Astrocytes support the normal operation of neuronal circuitry, regulating the extracellular potassium concentration and the clearance of synaptically released glutamate. Aside from the supportive roles of astrocytes, the hypothesis that astrocytes can modulate information processing in neuronal networks has been proposed. This view has gained some support by intense research in the past decades using *in vitro* experiments - either by use of cultured cells or acutely prepared brain slices - that revealed cytosolic Ca^{2+} dependent release of transmitter substances from astrocytes. In an attempt to investigate neuron-glia interactions in more intact conditions, we have been trying *in vivo* approaches using electrophysiology and two-photon optical imaging techniques in rodents.

Results and discussion. Extracellular recording using microelectrodes can measure local field potential and action potentials, reflecting the input and output activities of the neuronal network, respectively. Multi-site extracellular recording is a practical and powerful approach to compare neuronal network dynamics of genetically modified animals *in vivo*. In order to investigate astrocytic involvement of neural activity modulation, we investigated neural dynamics in mice with genetic interventions targeted to astrocytes. More specifically, we have been focusing on neural dynamics in mice that lack S100B, a major Ca^{2+} binding protein predominantly expressed in astrocytes.

We found a significant reduction in the amplitude of kainate-induced gamma oscillations (30-80 Hz) in the hippocampal CA1 str. radiatum of these mutant mice. Typical EEG patterns, such as cortical slow oscillations (0.5-2 Hz), hippocampal theta oscillations (5-10 Hz) and sharp wave-associated ripples (140-200 Hz), were not affected (Sakatani et al., Europ. J. Neurosci. 2007). We subsequently found that the S100B protein is secreted in a neural activity dependent manner. Furthermore, we demonstrated that activation of metabotropic glutamate receptor 3 (mGluR3) leads to secretion of S100B from astrocytes. S100B is known to be a ligand of the receptors for advanced glycation end-products (RAGE). In vivo antibody blockade of RAGE, and RAGE-KO mice, both demonstrate a role for RAGE in the modulation of gamma oscillations. While previous work had shown astrocyte to neuron communication to be mediated by small-molecule gliotransmitter release, such as of ATP or glutamate, our data demonstrate that astrocyte to neuron communication can also be mediated by secretory proteins [1].

Next, we investigated the activity patterns of cerebral cortical astrocytes *in vivo*. The cerebral cortex is composed of layers with unique cytoarchitecture. Astrocyte density varies among layers, yet the dynamical properties of astrocytic activity in different layers of the cortex were unknown. First, we performed *in vivo* intracellular recordings from cortical astrocytes to show that resting membrane potentials of histologically identified astrocytes are alike [2]. Next, using bolus loading techniques to label neurons and glial cells with Ca^{2+} sensitive fluorescent dyes *in vivo*, we investigated Ca^{2+} dynamics of astrocytes in mature (>P28) cerebral cortex by two-photon microscopy. This was a complementary study to our earlier study [3] which investigated similar questions in juvenile rats. We addressed two specific questions: (1) Does cerebral cortical layer 1 astrocyte activity differ from that of layer 2/3? (2) Is astrocytic Ca^{2+} activity modulated by brain state? We found that layer 1 astrocytes are more prone to discharging spontaneous Ca^{2+} surges and that the proportion of Ca^{2+}-active astrocytes is twice that observed in layer 2/3. Interestingly, these spontaneous astrocytic Ca^{2+} surges in the somata were not influenced by surrounding neural activity in urethane anesthetized animals. Moreover, we demonstrated that Ca^{2+} fluctuations in microprocesses of astrocytes show distinct differences in layer 1 and layer 2/3 [4]. We are currently studying how these astrocytic Ca^{2+} events are relevant in information processing of a sensory circuit in the cerebral cortex involving the barrel area.

Acknowledgements. This work was supported by a Grant-in-Aid for Scientific Research on Priority Areas from the MEXT of Japan (grant number: 18053026) and RIKEN BSI intramural research funds.

References

1. S. Sakatani, A. Seto-Ohshima, Y. Shinohara, Y. Yamamoto, H. Yamamoto, S. Itohara, and H. Hirase, *J. Neurosci*., 2008, **28**, 10928-10936.
2. T. Mishima and H. Hirase, *J. Neurosci*, 2010, **30**, 3093-3100.
3. H. Hirase, L. Qian, P. Bartho, and G. Buzsaki , *PLoS Biology*, 2004, **2**, E96.
4. N. Takata and H. Hirase, 2008, *PLoS One*, **3**, E2525.

CLINICAL CARS COMBINED WITH TWO-PHOTON FLUORESCENCE AND SHG IMAGING

K. König[1,2]

[1]JenLab GmbH, Schillerstraße 1, 07745 Jena, Germany and Science Park 2, Campus D1.2, 66123 Saarbrücken, Germany, info@jenlab.de, www.jenlab.de
[2]Saarland University, Department of Biophotonics and Laser Technology, Campus A5.1, 66123 Saarbrücken, Germany, www.blt.uni-saarland.de

Abstract. We developed *in vivo* high resolution hybrid multiphoton tomography based on two-photon fluorescence, SHG, and CARS for small animal research, the *in situ* detection of pharmaceutical components and cosmetics as well as medical diagnosis of skin cancer. The tomographs employ picojoule near infrared femtosecond laser pulses, flying spot technology, and single photon counting. It provides optical biopsies with intratissue submicron resolution, picosecond temporal resolution, 10 nm spectral resolution and chemical fingerprints. Lipids, water, NAD(P)H, flavins, melanin, keratin, porphyrins, elastin, and collagen can be imaged without any labeling. Furthermore, the major fluorescent proteins and hundreds of exogenous markers can be detected with single photon sensitivity.

More than 2,000 volunteers and patients have been investigated in Australia, USA, Japan, and Europe. Major studies include the early detection of malignant melanoma, chemotherapeutical agents and sunscreen nanoparticles in the skin, as well as the input of smoking, UV radiation, and anti-aging drug.

Introduction

Two-photon effects were predicted by the PhD student Maria Goeppert 80 years ago, demonstrated by Kaiser and Garrett 50 years ago, and applied to microscopy by Denk, Strickler, and Webb in 1990. First clinical two-photon systems (multiphoton tomographs) were developed by the JenLab GmbH some years ago. Two-photon cellular autofluorescence and second harmonic generation of collagen can be detected with single-photon sensitivity and submicron spatial resolution in the skin. The flexible multiphoton tomograph MPTflex was recognized with the Prism Award for the best photonic product in the category Life Sciences in San Francisco in January 2011.

Recent developments

In 2010, *in vivo* clinical CARS has been realized to image intratissue lipids and water. For that purpose, the multiphoton tomograph DermaInspect received an add-on CARS module based on an OPO to provide a second NIR beam, a time-delay unit, and red-sensitive PMTs to realize CARS. Using that hybrid femtosecond laser system, collagen could be detected in the blue by SHG, NAD(P)H and elastin in the blue-green by two-photon fluorescence, and water and lipids in the red spectral range by CARS. The novel clinical device was used in a clinical study in the Charite, the European Unions largest hospital (Fig. 1–3).

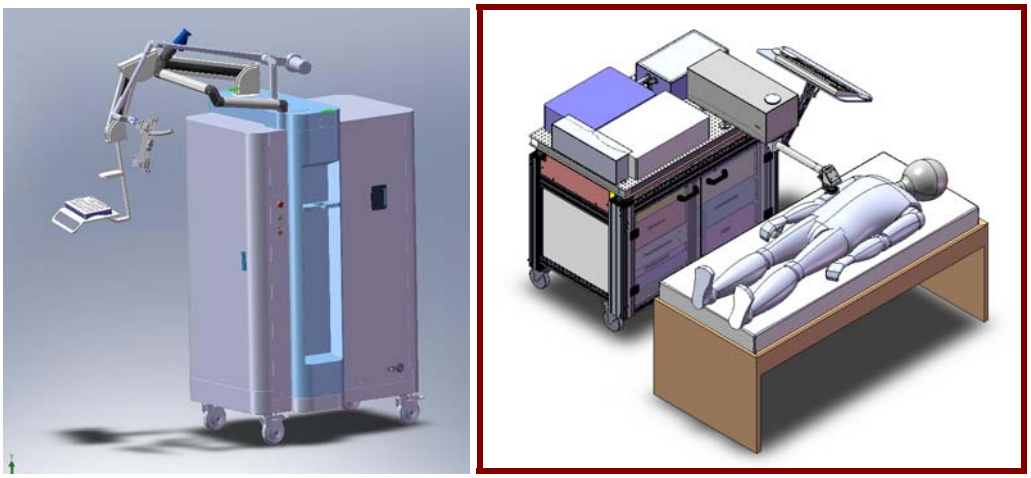

Fig. 1. Left: The Prism-Award winning multiphoton tomograph MPTflex for clinical use and small animal research. Right: Scheme of the tomograph DermaInspect-CARS

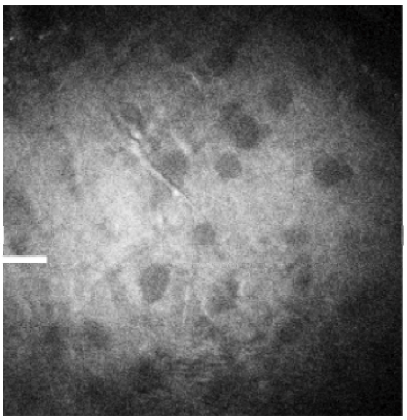

Fig. 2. Optical CARS section of a patient suffering from Psoriasis. Lipids are detected

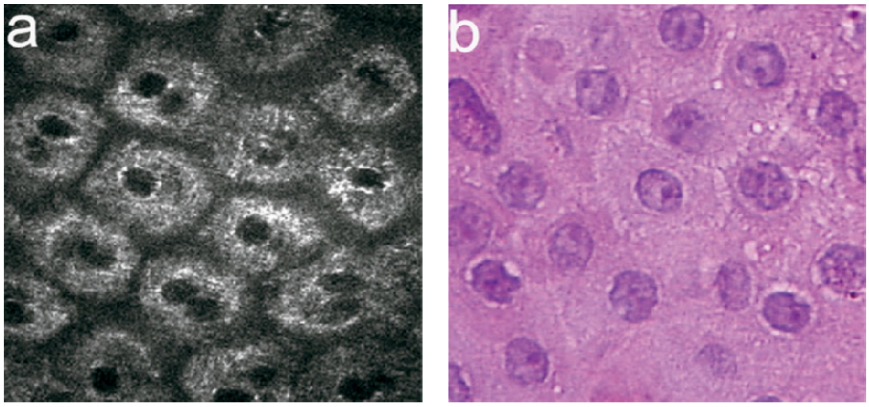

Fig. 3. Multiphoton tomographs provide *in vivo* images within seconds
with a better resolution than conventional pathology images of sliced and stained biopsies

In June 2011, a second clinical CARS tomography was introduced by JenLab based on a PCF supercontinuum.

Conclusion

Multimodal hybrid multiphoton imaging can be performed on cells, live animals and even humans to generate optical tissue biopsies with subcellular resolution, deep-tissue information, and chemical fingerprints. Novel multimodal multiphoton/CARS tomographs may become important biopsy-free and label-free imaging tools in personalized medicine, pharmacy, biotechnology, small animal research as well as cosmetic research.

References

1. König et al, "Optical skin biopsies by clinical CARS and multiphoton fluorescence/SHG tomography", *Laser Phys. Lett.*, 2011, DOI: 10.1002/lapl.201110014.
2. König et al., "Applications of multiphoton tomographs and femtosecond laser nanoprocessing microscopes in drug delivery research", *Advanced Drug Delivery Research,* 2011, doi:10.1016/j.addr.2011.03.002 .

DEVELOPMENT OF LASER DRIVEN CANCER THERAPY MACHINE

K. Kondo

Kansai Photon Science Institute, Japan Atomic Energy Agency, Kyoto, Japan
kondo.kiminori@jaea.go.jpl

Introduction

Recent laser technology enables us to generate PW class laser with 0.1 Hz as is demonstrated by GIST in Korea [1], while the same class high peak power laser pulse (called "J-KAREN") has been generated with the single shot base at JAEA in 2003 [2]. By focusing these ultrashort high peak power laser pulses, the extremely optical high field, of which normalized vector potential $\mathbf{a}_0$ becomes much larger than 1, can be generated in the laboratory. In such an extremely high field, the electrons move ponderomotively with the ultrarelativistic speed. Simultaneously, the accelerated electron bunch is kicked out from the focused area by the extreme photon pressure. When the target is a thin solid foil, the extremely high electric field is generated at the rear side of the foil, which accelerates protons existing as a contamination at the rear surface of the target. In 2000, by using the first PW laser system in the world, 60 MeV protons were successfully generated by this mechanism, which is called TNSA (Target Normal Sheath Acceleration) [3]. As is described above, in JAEA, the table top size PW laser system has been developed with tens of femtosecond pulse width, which corresponds to PW pulse generation with comparatively small output energy and small equipment size. Then from 2007, the project of photo medical valley creation was started in JAEA. In this project, the main aim was the development of laser driven particle cancer therapy machine. In this paper, the summary of the development will be presented. Especially, the recent experimental results of laser driven ion acceleration in JAEA are shown.

Laser driven ion acceleration experiments

In this development, the key issue is the successful acceleration of ions to over 200 MeV/u at least by using laboratory size laser system. The stopping range in water should be □20 cm for attacking deep inside the body. Then the required energy should be over 200 MeV for proton beam at least. In JAEA, ion acceleration experiments have been held with J-KAREN laser system, which is the PW class table top laser system in JAEA. Although in 2003 the peak power of J-KAREN once amounted to 0.85 PW, the actual irradiation peak power on target was not still so high. In order to improve this situation drastically, recently, the coupling efficiency between the output of J-KAREN and the real irradiation on the target has been improved. As a result, the irradiation intensity reached 4×10^{20} W/cm^2 with the extremely high contrast of over 10^{10} [4]. By this improvement, the detected maximum proton energy reached 23 MeV which is shown in Fig. 1. However, for 200-MeV generation, the higher intensity is found to be required with using the present tendency.

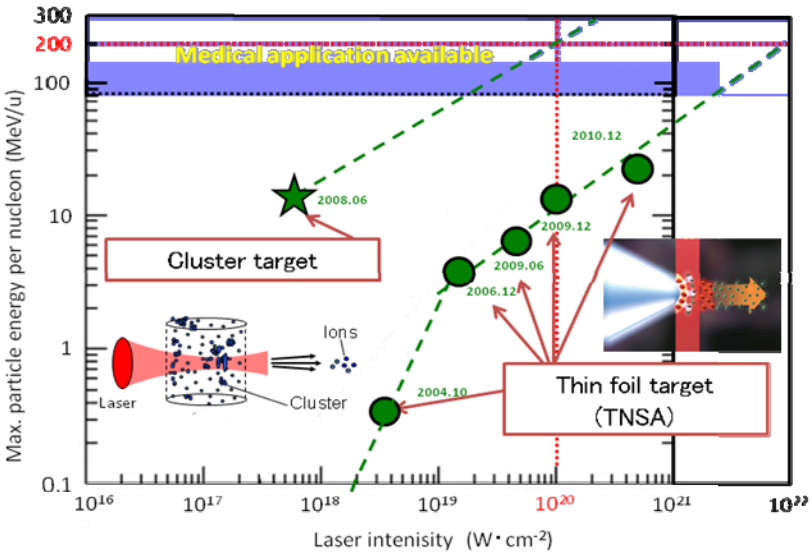

Fig. 1. Accelerated ion energy vs peak irradiation intensity

To improve this condition, some other ion acceleration approach has to be used. One of the approaches in JAEA was a method of using cluster target. In Fig. 1, there is a very high efficient plot,

which is over one order of magnitude higher than the trend of TNSA with femtosecond pulse obtained also in JAEA [5]. The dotted line which passes the star dot in Fig. 1 is proportional to square root of the irradiation intensity.

The obtained results with cluster target tell us the possible design of 200 MeV/u ion generation with the irradiation intensity of □1×10^{20} W/cm^2. For cluster target, the focusing of the pump pulse requires the f-number larger than 10. Then the required peak power for generating 200 MeV/u is proved to be 100 TW.

REB estimation with human cancer cell

Not only achieving high accelerated energy, but the starting actual cancer therapy test is also important in the development. When we use J-KAREN without pumping the final booster amplifier, 1 Hz operation is possible. In this mode, a few MeV quasi-mono energetic proton beam can be delivered with the chicane magnet shown in Fig. 2. By placing the human cancer cell samples at the exit of this chicane, a comparatively stable dose can be obtained. With this apparatus, relative biological effectiveness at 10 % survival fraction was measured to be 1.20 ± 0.11 with 2.25 MeV laser driven proton beam [6].

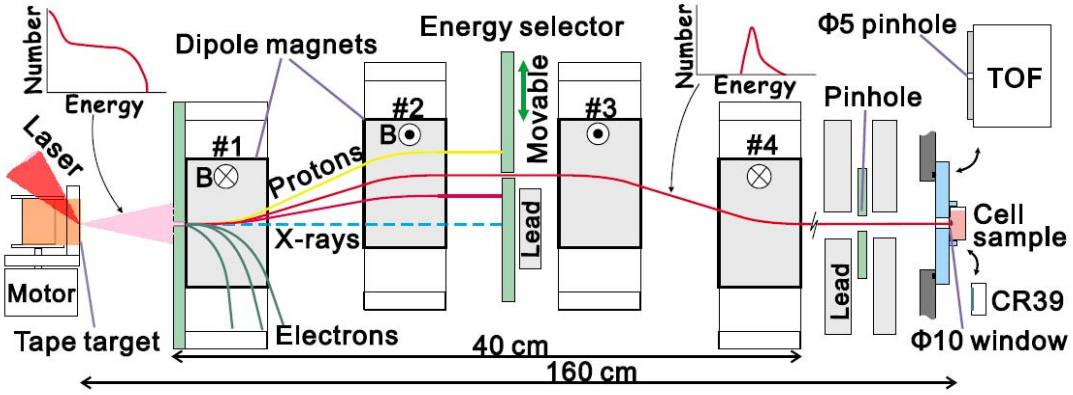

Fig. 2. Laser-driven quasi-mono energetic proton beam line

Acknowledgements

I would like to acknowledge all the related researchers and technical stuff in QuBS and KPSI in JAEA for having a fruitful research. Almost part of this work was performed in PMRC (Photo Medical Research Center), then I would also like to present my appreciation to our collaborator companies of PMRC (Toshiba, Hamamatsu photonics, Ushio, Shimazu, NAT, and HITZ), and HIBMC (Hyogo Ion Beam Medical Center).

References

1. J. H. Sung, et al., *Opt. Lett*., 2010, **35**, 3021.
2. M. Aoyama, et al., *Opt. Lett*., 2003, **28**, 1594.
3. R. Snavely, et al., *Phys. Rev. Lett*., 2000, **85**, 2945.
4. H. Kiriyama, et al., *Opt. Lett*., 2010, 35, 1497.
5. Y. Fukuda, et al., *Phys. Rev. Lett*., 2009, **103**, 165002.
6. A. Yogo, et al., *Appl. Phys. Lett*., 2011, **98**, 053701.

LAPARASCOPIC AND ENDOLUMINAL LASER TREATMENTS

R. Sroka[1], M. Hemmerich[1], C.G. Schmedt[2], and **W. Khoder[3]**

[1] Laser-Research Laboratory, LIFE-Centre at Ludwig-Maximilians University Munich, Munich, Germany
Ronald.Sroka@med.uni-muenchen.de
[2] Dept. of Phlebology, Diakonie-Klinikum, Schwäbisch-Hall, Germany
[3] Dept. of Urology, Ludwig-Maximilians University Munich, Munich, Germany

Clinical medical laser application using high power laser light offers the opportunity to destruct malignant and benign soft and hard tissue. Innovative developments in clinical endoscopic techniques allow for delivering high power laser light of up to 200 W in continuous wave manner or 2 J/pulse by single fibres. Laparascopic continuous wave laser invention in urology for partial tumor nephrectomy by means of bare fibre technique without ischemia would be beneficial for the patient. While single case descriptions are available, clinical studies with respect to the duration of ischemia are missing. Endoluminal laser treatment of incompetent great saphenous veins of patients suffering from varicosis is a promising new procedure offering fewer side-effect compared to conventional surgical stripping methods, but the possibilities of feedback guidance of this procedures are not available. Here, a method of on-line temperature monitoring within the vessel in the region of interest will be presented.

Laser assisted laparascopic partial tumor nephrectomy without renal hilar clamping

Recent clinical surveys revealed increasing incidental detection of renal cell carcinoma partly due to widespread use of imaging procedures as ultrasonography, computed tomography, and magnetic resonance imaging [1, 2]. This has led to a shift in the surgical management of renal carcinoma toward widening the indications for nephron sparing surgery. Laparoscopic techniques for partial nephrectomy are well described [3]. Haemostasis represents the important challenge during this procedure so that clamping of renal vasculature is often necessary to allow precise tumour removal in a bloodless field. The consequent warm ischemia places significant time constraints on the surgeon during tumour excision and parenchymal reconstruction adding further technical challenges to the procedure [3]. The aim of the current prospective study was to evaluate and establish an *in-vivo* laser laparascopic partial nephrectomy technique without renal hilar clamping.

A semiconductor diode laser (Eraser, Rolle&Rolle, Salzburg, Austria) emitting light at wavelength of 1318 nm in a cw mode was used. Laser output power could be set between 1 and 100 Watt. The light is coupled into a flexible bare ended laser fibre. This fibre was introduced into a specially designed commercially available guidance instrument [4] (Karl Storz, Tuttlingen, Germany) during laparascopic interventions. This fibre guidance instrument allows for controlled bending of the distal fibre tip between -5^0 and 50^0. Furthermore, an irrigation system was attached to enable rinsing of the incision site to improve the direct vision and cutting efficacy.

Thirteen patients were included in a prospective feasibility study of diode-laser partial tumour-nephrectomy. All patients suffered from a suspected malignant renal mass of unknown histology which had been incidentally found in routine US and subsequent CT and were candidate for partial nephrectomy. All patients gave an informed consent after being given detailed information about the planned procedure. The study was approved by the Ethics Committee of the Faculty. As a first step the technique was established during open surgery (n = 5) to standardise the manoeuvres and manage/define perioperative complications followed by laparascopic approaches (n = 8)**.**

The basic experimental part revealed that laser adjustment between 45–70 W in a moderate cut velocity (1–3 mm/second) is sufficient for adequate manipulations (cutting as well as preparation). Logically, with slow cut velocity, the coagulation zone becomes deeper (up to 4 mm) rather than with fast cutting where coagulation effect is almost lost. Dissection of vessels and pelvicalyceal system was feasible. Heavy smoke appears if the laser application continued more than one minute per application.

The mean operative time (skin to skin) was 116.5 minutes (ranging from 60 to 90 min for open surgery and 110 to 175 min for the laparascopic approach) with mean estimated blood loss of 240 ml (50 to 600 ml) with no real differences between open compared to laparascopic approach. The laser activation time for tissue removal was 7 to 13 min during open surgery and 9 to 17 min during the laparascopic intervention.

There was no need for conversion from laparascopic approach to open surgery. Two patients needed vascular clamping with an average duration of 21.5 minutes. There were no peri-operative complications. 2 patients developed post-operative fever which was not surgery-related. Histologically, the coagulation depth ranged from < 1 to 2 mm without limiting the histological evaluation of tumours or resection margin. 3 months follow-up-CT showed normal kidney size and function without tumour recurrence. In-vivo experience confirmed experimental results that smoke obscuring laparascopic vision developed if the laser was activated for > 1 minute per application. In case of bleeding, suction of blood in combination with water irrigation is mandatory for adequate laser coagulation. Follow up ranged from 3–6 months. One patient developed an A-V fistula after one month which was successfully embolized. Otherwise, all patients showed uneventful follow up examinations.

Temperature measurement during endoluminal laser treatment of varicosis veins

During the last decade a variety of endoluminal treatment modalities for insufficient varicosis veins were technically developed, experimentally investigated in ex-vivo and in-vivo experiments, and finally introduced into the clinical treatment options. Endoluminal techniques are medical approved and the clinical improvement of endoluminal treatments are accepted by physicians, due to recent meta-analysis of large cohort studies, as well by the patients. Unfortunately, there are still questions about a certain feedback giving the potential of control or immediate hints for the success of the treatment. With respect to this, a temperature measuring system which can be used in high intensity electro-magnetic field without self heating and without giving artefacts to potential image systems (e.g. US, MRI, CT) was developed and tested.

The physics of the temperature sensor is based on the optical properties of a ruby-crystal which is normally used as active material of a ruby laser, here the optical emission of photons due to the main transition and a broad spectrum based on thermally induced fluorescence in used [4–6]. The sensor head consists technically of a ruby-hemisphere coupled to a polished flat top ended optical fibre. The ruby-fluorescence was excited at 532 nm. The induced ruby-fluorescence was guided back via the same optical fibre and after leaving the fibre at the proximal end it was deflected by means of a beam splitter onto the entrance of spectrometer. The detected fluorescence spectrum showed a broad fluorescence in the spectral range of 620 to 750 nm with its prominent R-line aT 694.2 nm. The intensity of the complete spectrum is temperature dependent but in different manner for the R-line area and the broad fluorescence spectrum. Thus, the temperature dependent evaluation needs the ratio of the integral R-line intensity between 690 and 700 nm subtracted by the fluorescence background in this spectral region an the complete integral intensity of the fluorescence spectrum subtracted by the R-line fluorescence estimating a homogenous intensity of the background.

The functionality of this temperature sensor within the EM-field of laser light was tested in the ox-foot-model [8] as on-line monitoring during endoluminal treatment. Ox-foot-model veins were rinsed and filled with heparinized blood. A newly developed radial emitting fibre and a temperature sensor was coupled and fixed together that the sensor head was proximate fixed to the glass dome of the fibre and directly within the irradiation pattern of the fibre and introduced into the vein. Before starting the treatment the control of the position was performed. During the experimental testing the developed device worked in a suitable manner. The time courses of the endoluminal temperature measurement parallel to radial emitting treatment fibre, 6 W at 1470 nm, showed an temperature increases up to 100°C during pullback. After heating up a constant temperature for the time of treatment and pulling could be derived, thus the parameter 6 W and 1 mm/s pull velocity resulted in a equilibrium. This way a total LEED of 60 J/cm was applied which induced shrinkage of the vein tissue realized either by observation but also by the sensation of increased adhesion between fibre and tissue during continuous steady going pulling. An increase of the laser output laser power to 10 W resulted in a maximum temperature of $T_{max} = 145°C \pm 20°C$. Tightening sensations occurs strong accompanied with abrupt relaxation and the related temperature jumps. The macroscopic evaluation of the intima showed dark coloured stripes at the position of tightening but without carbonization.

By means of the presented special designed temperature sensor based upon the temperature dependent fluorescence of the ruby crystal could solve the problem of temperature measurement in the irradiation field as no interaction with the treatment laser light such as absorption and self heating could be observed. A temperature accuracy of ±2°C in the 100°C range is reliable for the endoluminal dedication. Adhesion

effects could be verified by the temperature time course. Testing this device showed that by means of such a physical sensor a more controlled energy application could be achieved.

Conclusions

The described preliminary results of the 1318-diode laser partial nephrectomy showed that the technique is feasible, adherent to surgical standards and add benefits to both laparoscopic as well as open techniques without compromising the oncological results. Developments are needed to optimise the laser fibre guidance instrumentations as well as to find the optimal laser equipment [8].

Control and considering physical parameters such as the pull back velocity of the treatment fibre and the irradiation parameters (e.g.. EFE, LEED) and additionally the local endoluminal temperature serve for improved reliable and successful treatment for the benefit of patient. Further developments in on-line in-situ measurement of the local temperature could result in a more reliable and controllable treatment potential. This way the endoluminal treatment procedures of varicosis vein should be improved for the benefit of the patient as well as under socio-economic aspects.

References

1. A.J. Pantuck, A. Zisman, A.S. Belldegrun, *J. Urol.,* 2001, **52**, 447-50.
2. W.H. Chow, S.S. Devesa, J.L. Warren, J.F. Fraumeni Jr., *JAMA*, 1999, **281**, 1628-31.
3. B.R. Lane, I.S.Gill, *J. Urol.,* 2007, **177**, 70-4.
4. R. Sroka, P. Rösler, P. Janda, G. Grevers, A. Leunig, *Laryngoscope,* 2000, **110**, 332-4.
5. K.T.V. Grattan, R.K. Selli, A.W. Palmer, *Review of Scientific Instruments,* 1987, **58**, 1231-1234.
6. W.H. Fonger, C.W. Struck, *Phys.Rev.B*, 1975, **11**, 3251-3260.
7. H.C. Seat, J.H. Sharp, Z.Y. Zhang, K.T.V. Grattan, *A-Physical*, 2002, **101**, 24-29.
8. C.G. Schmedt, O.A. Meissner, K. Hunger, G. Babaryka, V. Ruppert, M. Sadeghi-Azandaryani, B.M. Steckmeier, R. Sroka, *J. Vasc. Surg.,* 2007, **45**, 1047-1058.
9. O.L. Antipov, N.G. Zakharov, M. Fedorov, N.M. Shakhova, N.N. Prodanets, L.B. Snopova, V.V. Sharkov, R. Sroka, *Medical Laser Application* 2011, **26**, 67–75.

FEMTOSECOND AND NANOSECOND LASER NANOSURGERY: NEW PERSPECTIVES FOR CONTROLLED NONLINEAR ENERGY DEPOSITION

A. Vogel, N. Linz, S. Freidank, X. Liang, S. Eckert, and **J. Noack**

Institute of Biomedical Optics, University of Luebeck, Peter-Monnik Weg 4, 23562 Lübeck, Germany
e-mail: vogel@bmo.uni-luebeck.de

Tunable nonlinear energy deposition in a large parameter range

Using a novel experimental technique that detects transient laser effects as small as 50 nm [1], we demonstrate that low-density plasmas and nanoeffects can be produced not only using ultra-short laser pulses but also, in a much more cost-effective way, by means of temporally smooth *nanosecond* pulses of short wavelengths [2]. We also show that luminescent plasmas of high energy density are formed when tightly focused femtosecond pulses of > 100 nJ pulse energy are focused into transparent materials, and determine plasma pressure and temperature [3]. Controlled nonlinear energy deposition with widely tunable energy densities is, hence, possible in a large part of the parameter space spanned by wavelength (UV to IR) and pulse duration (fs to ns). Only ns breakdown at IR wavelengths is intrinsically characterized by an abrupt jump from 'no absorption' to brightly luminescent, dense plasma. The tunability opens exciting perspectives for laser material processing, precision manufacturing, and surgery of cells and tissues.
We demonstrate the *tuning* of nanosecond laser effects from nanoeffects to larger, disruptive effects on various examples ranging from bubble formation in water through photoporation of cells and cavitation in corneal tissue to the creation of refractive index changes or voids in glass.

Model of plasma formation including temperature evolution and thermal ionization

Modeling of controlled nonlinear energy deposition requires a change of paradigms: it is no longer sufficient to determine breakdown thresholds but one needs to be able to calculate the dependence of energy density and material temperature from laser parameters to assess the resulting phase transition and ablation effects. We present a model that fulfils these requirements. Besides considering photoionization, avalanche ionization, recombination, and diffusion losses, it also considers heating through residual linear absorption and via collision losses and recombination of the free electrons produced by nonlinear absorption, as well as its counteraction by heat diffusion out of the focal volume. Sufficiently high temperatures result in thermal ionization accelerating the ionization avalanche.

The predictions of the advanced model are in excellent agreement with our experimental results achieved with fs, ps and ns pulses at various wavelengths from 347 to 1064 nm. The good agreement encouraged creating a map of the (λ,τ) parameter space in which the dependence of target temperature on laser energy is calculated for each (λ,τ) value. This 'tunability' map for the magnitude of laser effects is very useful in guiding the choice of laser parameters for a large variety of applications.

Application of UV nanosecond laser pulses for flap dissection in refractive surgery

Together with an industrial partner, we developed a clinical device for the cutting of flaps for refractive surgery (LASIK). The precision of cuts in porcine cornea performed by 355-nm, 1-µJ pulses at 150 kHz repetition rate is better than with IR femtosecond laser pulses focused at the same NA because focus diameter and length are only one third of the values at 1064 nm.

Acknowledgements

The basic research was supported by the US Air Force Office of Scientific Research (AFOSR). The applied research was conducted jointly with Schwind Eye Tech Solutions, and supported by the German Ministry of Economy (BMWi) through "Zentrales Innovationsprogramm Mittelstand" (ZIM).

References

1. A. Vogel, N. Linz, S. Freidank, G. Paltauf, *Phys. Rev. Lett.*, 2008, **100**, 038102.
2. A. Vogel, N. Linz, S. Freidank, J. Noack, G. Paltauf, *Tutorial at CLEO 2008*, 3-page summary in OSA Technical Digest, paper: CMHH1, 2008.
3. A. Vogel, N. Linz, S. Freidank, G. Paltauf, Invited Talk at CLEO Europe 2009.